PCCP

PAPER

Cite this: *Phys. Chem. Chem. Phys.*, 2016, **18**, 9396

Effects of tensile strain on the peculiarities of PEO penetration into the nanoporous structure of PET deformed *via* the crazing mechanism

E. G. Rukhlya,* L. M. Yarysheva, A. L. Volynskii and N. F. Bakeev

Received 18th December 2015,
Accepted 28th February 2016

DOI: 10.1039/c5cp07842c

www.rsc.org/pccp

Solvent crazing involves the development of a highly dispersed fibrillar-porous structure with dimensions of pores and craze fibrils of about 2–20 nm, and crazing by itself can be treated as a universal method for the development of nanoscale porosity. The penetration and release of poly(ethylene oxide) macromolecules into and from the crazes during the development of the nanoporous structure of poly(ethylene terephthalate) have been studied. In particular, PET has been deformed in dilute or semidilute (unentangled as well as entangled) solutions of PEO (a M_w of 4 and 40 kDa) *via* the mechanism of solvent crazing. Hydrodynamic coil radii R_h, blob sizes ξ, and concentration ranges (crossover and entanglement concentrations) have been determined for the PEO solutions. The evolution of the craze structure (change in porosity W and pore diameters d) has been described as a function of the tensile strain of PET during its drawing in an adsorption-active medium and in the PEO solutions. PEO has been shown to penetrate into the nanoporous structure of the crazes under the conditions corresponding to $R_h \leq d$ and $\xi < d$. It has been shown that coagulation processes in the structure of crazed PET, PEO adsorption at the highly developed surface of PET, and the mechanism of PEO transport in the nanopores are equally important factors affecting the direction of the macromolecule mass transfer in the nanopores (penetration or release) and PEO content variation as a function of PET tensile strain.

1. Introduction

The penetration of macromolecules into nanopores is a complex physicochemical phenomenon. Its special feature is that very often the penetration is possible even though the macromolecular coils are larger than the pores.[1–8] In recent years, increasing attention has been focused on studies of the peculiarities of macromolecule penetration into diverse nanoporous materials, such as porous glasses,[7,9–12] track membranes,[2,13–17] protein nanopores[5,8,18,19] and protein nanochannels.[20–23] Crazing in liquid media[24–26] is a universal method for imparting nanoscale porosity to polymer films and fibers. Crazing consists of the self-dispersion of a polymer under the combined action of tensile stress and adsorption-active medium (AAM) affording nanosized aggregates of oriented macromolecules (fibrils) spatially separated with voids of nearly equal size. The porosity development in the course of crazing is accompanied by the penetration of the surrounding liquid into the nanoporous structure being formed. The feature of simultaneous development of the pores in the drawn polymer and their filling with the solution underlies the original method of polymer-based nanocomposite production taking advantage of crazing.[27–29] In the above-cited studies, polymer deformation *via* the crazing mechanism in the solutions of various low-molecular weight compounds has been addressed.

Our earlier reports[30–33] were the first to demonstrate the possibility of deformation of a glassy polymer, poly(ethylene terephthalate) (PET), in a semidilute solution of another polymer, poly(ethylene oxide) (PEO), *via* the mechanism of solvent crazing, which allows obtaining polymer–polymer blends with a high level of mutual dispersion between the components. Special features of polymer deformation in a solution of a high-molecular compound are as follows.[30–33] (1) PET deformation in semidilute solutions of flexible-chain PEO is accompanied by the formation of nanosized pores and efficient penetration of PEO into the pore space. (2) The amount of PEO in the crazed PET is markedly larger than that calculated assuming that the PEO concentrations in the solution filling the PET pores and in the surrounding solution are equal. The excessive content of PEO can be attributed to its adsorption at the highly developed surface of the fibrillized polymer in the crazes. (3) PEO penetration into the pores of PET being developed *via* the crazing mechanism is enormously fast, occurring within minutes of the drawing. At the same time, the equilibrium is attained much slower, within days, in the course of PEO diffusion

Faculty of Chemistry, M. V. Lomonosov Moscow State University, Leninskie gory 1, Moscow 119234, Russia. E-mail: katrin310@yandex.ru

 This journal is © the Owner Societies 2016

into a pre-formed matrix of the crazed polymer. Noteworthily, the above-listed peculiarities are common for penetration of flexible-chain macromolecules into the nanoporous structure of polymers being deformed *via* the crazing mechanism; they have been observed upon drawing various amorphous (glassy) and crystalline polymers.[31,34,35] Therefore, crazing of polymers in solutions of high-molecular compounds may be considered a simple and universal method to prepare the finely dispersed polymer–polymer blends.

Importantly, the same PET deformation strain was applied in the above-mentioned studies of PEO transport into the nanoporous crazed PET; therefore, parameters of the porous structure are similar. However, the nanoporous structure evolution during the crazing deformation of a polymer in an AAM is a complicated process. Initially, crazes with their unique fibrillar porous structure start to grow in the direction perpendicular to the direction of the applied stress crazes. Once the initiated crazes pass through the whole cross section of the sample, the stage of craze thickening comes when the growing crazes increase their width along the direction of tensile drawing. At this stage, the starting bulk polymer is continuously transformed into a finely disperse ''substance'' (oriented (fibrillized) state) composed of crazes. However, at some point this process becomes unfavorable, and the excess surface area should be somehow decreased. Therefore, at a sufficiently high tensile strain, when a substantial part of the polymer has been transformed into the oriented fibrils, collapse of the porous structure starts, accompanied by transversal contraction of the polymer. The contraction results in decrease of porosity, average pore size, and specific surface area of the material.[24,36]

In this work, we elucidated the influence of the structure evolution during PET crazing in solutions of PEO on the macromolecule penetration into the formed pores. To do so, we studied the effects of PEO molecular mass and concentration (in particular, dilute, semidilute unentangled and semidilute entangled water–ethanol solutions of PEO were used) on the mechanism of PEO penetration into the PET material being deformed up to the fibrillar-porous structure collapse at high tensile strain.

2. Experimental

2.1 Materials

Amorphous non-oriented polyethylene terephthalate (PET) films with a thickness of 100 μm were used as the matrix. Poly(ethylene oxide) (PEO) with a molecular mass of 4 kDa (PEO4K) or 40 kDa (PEO40K) was used as the flexible-chain component (both from Aldrich; the polydispersity index of 1.1) for penetration into the solvent-crazed PET. Tensile drawing of PET was carried out in the ethanol–water (7 : 1 by volume) solutions of PEO. A water–ethanol mixture (1 : 7, v/v) was chosen as the adsorption-active medium, since ethanol is adsorption-active towards PET and facilitates the development of deformation *via* the crazing mechanism. Water is inert towards PET; however, its presence ensured the solubility of PEO.

2.2 Sample preparation

PET–PEO blends. High-molecular PEO is solid at room temperature; therefore, it can only be incorporated into the PET film being deformed *via* crazing from the solutions. The PET samples with a gauge size of 6.15 × 20 mm immersed in a PEO solution in the water–ethanol (1 : 7 v/v) mixture were stretched at a constant strain rate of 5.4 mm min^{-1}. The PEO concentration in the solution was varied from 5.5 to 30 (w/v)% (from 5.5 to 30 g for 100 mL solution). The solvent-crazed samples (PEO–PET blends) were wiped off in order to remove the residual PEO from the surface and then dried under isometric conditions until their weight was constant to remove residual solvent. The content of PEO in the blends was estimated gravimetrically.

Sample for the experiments of PEO diffusion into the pre-crazed PET under the concentration gradient. The PET films immersed in the water–ethanol (1 : 7 v/v) mixture were stretched at a constant strain rate of 5.4 mm min^{-1}. The stretched samples were fixed in the clamps without removal of the solvent, immersed in the 20% PEO solution, and incubated under isometric conditions (preventing shrinkage).

2.3 Calculation of porosity

Porosity W of the solvent-crazed PET was defined as the penetration volume change $\frac{\Delta V}{V_0} = \frac{V_t - V_0}{V_0} \times 100\%$, with ΔV being the increase of the specimen volume after its tensile drawing given the tensile strain, and V_0 standing for the initial specimen volume.

2.4 Content of PEO in PET

The content of PEO was determined by weighing and is defined as $\frac{\Delta m}{m_0} = \frac{m_t - m_0}{m_0} \times 100\%$, with m_0 being the initial mass of a PET specimen and m_t standing for its mass after deformation in a PEO solution and after removing the solvent.

2.5 Calculation of the theoretical content of PEO in porous PET

The theoretical content of PEO was estimated assuming that the surrounding PEO solution was merely filling the whole pore volume without any change in the concentration. Then the PEO content could be calculated as follows: $\frac{\Delta m}{m_0} = \frac{cW}{(1-W)\rho} \times 100\%$, with c being the PEO solution concentration, ρ being the PET density, and other symbols having the same meaning as in the above equations.

2.6 Pressure-driven liquid permeability

Effective pore dimensions for the PET sample stretched by 100–300% in the ethanol–water solution were calculated according the procedure described in ref. 37 from the data on volume porosity and pressure-driven liquid permeability. To gain information on pore dimensions for the ''native'' solvent-crazed samples (or, in other words, for the samples whose

structure remains virtually unchanged after their tensile drawing), the solvent was not removed from the solvent-crazed samples and their contour was fixed by an O-shaped metallic framework in order to prevent any shrinkage. Liquid permeability through the porous samples was measured using an FMO-2 membrane cell at a pressure of 2 MPa with respect to the same water–ethanol solutions, in which tensile drawing *via* solvent crazing was performed. The cell was modified in a way enabling the measurements in the presence of a liquid medium, under the conditions preventing the specimen shrinkage after drawing. Thus, the effective pore diameter determined *via* that method reflected the ''native'' structure of the crazed PET. The effective pore size (r) in the crazes was calculated from the data on the liquid permeability (G) and porosity (W) of the solvent-crazed samples using the Pouseille equation: $G = \frac{Wr^2 S_0 \Delta P}{8\eta d}$, with ΔP, the external pressure; d, the film thickness; η, the liquid viscosity; and S_0, the film area.

2.7 Viscosity

The penetration viscosity of the PEO solutions in a water–ethanol mixture was measured using an Ubbelohde viscometer (viscosity of the mixed solvent was of 2.33 cps; no corrections for kinetic energy was made). Prior to the measurements, all solutions were incubated at 20 °C for 15 min; the temperature was maintained within ±0.2 °C.

2.8 Light scattering

Light scattering of the PEO solutions was measured using a Photocor Complex photometer (Photocor Instruments, USA) equipped with a He–Ne laser as the light source (10 mW, λ = 633 nm, scattering angle of 90°). PEO concentration in the solutions was 0.7 wt%. The solutions were filtered through Millipore porous filters with a pore size of 0.2 μm. The hydrodynamic radius of the macromolecules R_h was calculated from the self-diffusion coefficient D data using the Einstein–Stokes equation: $R_h = \frac{kT}{6\pi\eta D}$, with k being Boltzmann's constant, T standing for the temperature, and other symbols having the same meaning as in the above equations.

2.9 Correlation length

The correlation length (ξ) for the PEO macromolecules in the water–ethanol solution was calculated using the equation for the flexible-chain polymers in a good solvent: $\xi = R_h\left(\frac{c}{c^*}\right)^{-\frac{3}{4}}$, with c^* being the crossover concentration (see below), and other symbols being explained as above.

2.10 Crossover concentration

We calculated the solutions' intrinsic viscosity [η] by extrapolation of the reduced viscosity to zero concentration. The crossover (or overlap) concentration c^* was calculated from the intrinsic viscosity data according to the Debye criterion: $c^* = [\eta]^{-1}$

2.11 Entanglement concentration (c^{**})

The entanglement concentration corresponding to the appearance of a network of entanglements involving all the macromolecules in a solution was determined from the inflection point in the plot of the solution reduced viscosity as a function of concentration.

3. Results and discussion

3.1 Characteristics of PEO solutions

Depending on the concentration, polymer solutions are classified into dilute, semidilute unentangled, semidilute entangled, and concentrated ones.[38,39]

Macromolecules exist as individual isolated coils in the dilute solution, and the polymer–polymer interactions are insignificant. It is commonly believed that the transport of macromolecules in nanopores from dilute solutions occurs *via* the translational mechanism, and the value of the hydrodynamic coil radius $R_h \leq d$ serves as a critical parameter. A different behavior is observed in the case of semidilute solutions. As the polymer concentration increases up to the crossover range (c^*), the individual chain motion cannot be considered independent anymore since the coils start to overlap and a fluctuating polymer network appears in the solution. The network mesh size, referred to as the correlation length (ξ), corresponds to the distance measured along a chain between two intermolecular contacts. According to de Gennes, a macromolecule of a flexible-chain polymer in the semidilute solution may be represented as a chain of blobs, its root-mean-square size corresponding to the correlation length ξ.[40,41]

The formation of the fluctuating polymer network starts at the crossover concentration c^* and continues up to the c^{**} concentration, the latter one marking the passage of the system to the semidilute entangled solution regime containing a network of the entangled polymer. At the polymer concentration in the solution of c^{**} the translation mechanism of the polymer diffusion is changed into the reptation one; the scaling concept states that the blob size $\xi \leq d$ should be used as a critical parameter.[40,42] Therefore, determination of the conditions for the flexible-chain macromolecules to penetrate into the nanoporous matrices required accounting for both the pore size and the concentration regime of the external polymer solution.

Thus, there are three regimes:

(1) dilute solution (macromolecules exist as individual isolated coils ($c < c^*$));

(2) semidilute unentangled solution (where the concentration is large enough to have some chain overlap ($c^* < c < c^{**}$) but not enough to cause any significant degree of entanglement);

(3) semidilute entangled solution (marks the distinct onset of significant chain entanglements in solution ($c > c^{**}$)).

The data on intrinsic viscosity [η], hydrodynamic coil radius R_h, crossover concentration c^*, entanglement concentration c^{**}, and the blob size ξ at different concentrations for the PEO used in this work are given in Table 1.

 This journal is © the Owner Societies 2016

Table 1 Characteristics of PEO in the water–ethanol (1 : 7 v/v) solution

PEO sample	$[\eta]$, dL g^{-1}	c^*, g/100 mL	c^{**}, g/100 mL	R_h, nm	ξ, nm at c = 5.5%	ξ, nm at c = 20%	ξ, nm at c = 30%
PEO4K	0.13	7.79	23.8	1.3	—	0.6	0.45
PEO40K	0.58	1.67	11.0	5.2	2.2	0.8	—

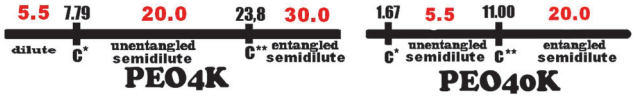

Fig. 1 Schematic concentration-state diagram of PEO solutions. The red labels show the polymer concentration in (w/v) % used in this work.

The data in Table 1 shows that the state of the PEO solution depends on the polymer molecular mass and concentration, as illustrated in Fig. 1.

Overall porosity and the pore diameter of the crazes are the parameters reflecting the porous structure of solvent-crazed polymers. When a polymer is deformed in a liquid media *via* the crazing mechanism, the material structure formed immediately in the course of the drawing (the so-called "native" structure) differs from that developing after the solvent has been removed.[24] Obviously, the parameters of the native structure of the crazes are those determining the possibility and regularities of PEO macromolecule penetration into the pores.

3.2 The dimensions of pores and porosity in the solvent-crazed PET films

The porosity ($\Delta V/V_0$) of the solvent-crazed polymer as a function of the tensile strain in the cases of water–ethanol mixture (curve 1) as well as 20% solutions of PEO4K (curve 2) and PEO40K (curve 3) in the same medium is collected in Fig. 2. Since the porosity was determined from the size of the films measured directly in the course of the drawing in the presence of the liquid media, the determined values corresponded to the native structure of the crazed polymer. Furthermore, Fig. 2 shows the theoretical porosity of PET as a function of the tensile strain (curve 4); that dependence was calculated assuming that the deformation occurred entirely *via* the crazing mechanism and was accompanied by a continuous increase in the polymer volume.

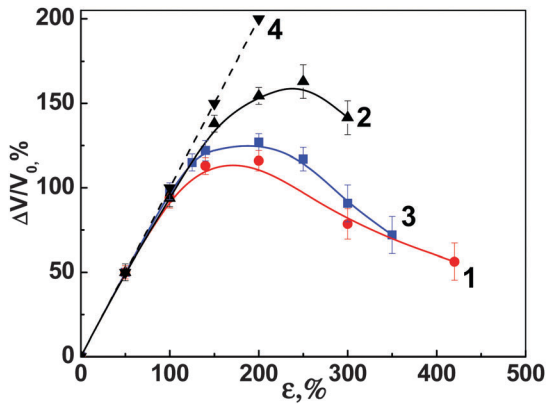

Fig. 2 Porosity of solvent-crazed PET in a water–ethanol mixture (1), 20% solutions of PEO4K in the same mixture (2), and 20% solution of PEO40K in the same mixture (3) at the drawing rate of 5.4 mm min^{-1} as a function of the tensile strain. Curve (4) shows the theoretical estimation of the porosity (see details in the text).

The results shown in Fig. 2 revealed that two ranges of the strain could be distinguished as far as the porosity evolution was concerned. At low tensile strain ($\leq$100%), the porosity of the solvent-crazed PET in the PEO-free as well as PEO-containing water–ethanol mixtures coincided with the theoretical estimation. In that case, the drawing occurred *via* the specimen elongation but was not accompanied by transversal contraction (in other words, in contrast to the case of shear deformation, the specimen width and thickness did not change upon deformation). At higher tensile strain ($>$150%) the situation was different: the solvent-crazed PET films in all the used liquid media exhibited a noticeable transversal contraction, consequently, the specimen porosity was lower as compared to the theoretical estimation. The presence of PEO in the solution had no effect on the qualitative behavior of the PET porosity as a function of the tensile strain. However, the porosity was somewhat higher in the presence of PEO in the AAM. Noteworthily, in the case of PEO4K the porosity was higher and decreased at higher tensile strain as compared with the case of PEO40K. Hence, PEO4K was a more efficient stabilizer of the crazed PET structure.

The porosity profiles 1–3 in Fig. 2 are typical of an amorphous glassy polymer being deformed in AAMs *via* the crazing mechanism; the behavior has been explained by the structural rearrangements of the fibrillar-porous structure of the crazes at high tensile strain due to the formation of coagulation contacts between the individual fibrils (see the scheme in Fig. 3).[24,36]

In particular, the structure evolution during a polymer deformation in an AAM can be rationalized as follows. At the initial stages of the drawing, crazes of a unique fibrillar-porous structure are nucleated in the polymer. The nucleated crazes grow in the direction normal to the drawing axis until they or their ensembles have grown throughout the specimen cross-section. Upon further drawing, the crazes widen and thicken. It is this stage of the craze development when the polymer passes into the oriented (fibrillized) state, and its porosity and specific surface area continuously increase. However, the finely dispersed fibrillar-porous structure of the crazes is thermodynamically unstable and tends to reduce the excess surface energy. As the tensile strain is increased, the intercraze regions

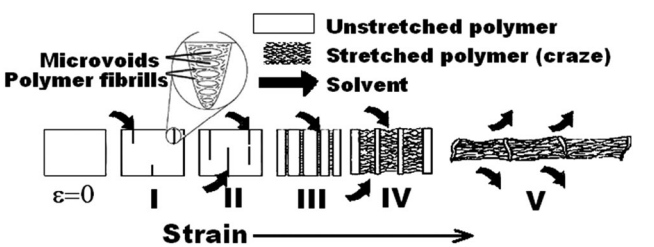

Fig. 3 Schematic representation of structural rearrangements accompanying polymer drawing in the AAM.

Table 2 Effective pore diameter of the crazes appearing in the solvent-crazed PET in the water–ethanol solution

ε, %	100	160	200	300
d, nm	7.8	8.2	6.2	3.8

of the non-deformed polymer that hinder the transversal contraction of the crazed polymer are consumed. Moreover, the fibrils connecting the opposite walls of crazes are elongated, thereby becoming more flexible and facilitating the formation of coagulation contacts between them. The combination of these processes reduces the overall porosity of the solvent-crazed polymer, as documented in Fig. 2.

In summary, the experimentally determined PET porosity values coincided with the theoretical estimation at the tensile strain of up to 100%, whereas at higher tensile strain the porosity was significantly overestimated, thereby indicating rearrangements in the crazes resulting in the collapse of their structure. Therefore, it was of interest to study the features of PEO macromolecule penetration into the nanoporous structure of crazes upon PET deformation, before and after the structural transformations relevant to the collapse of the fibrillar-porous structure.

The native structure of solvent-crazed PET in the AAM was characterized and the pore sizes were determined using the liquid penetration under the pressure gradient method in the presence of a liquid medium thus excluding the effect of the deformed specimen shrinkage. The effective pore diameters of crazes in the solvent-crazed PET to different tensile strains in the water–ethanol mixture are given in Table 2.

3.3 Features of penetration of the PEO macromolecules into the pores upon tensile drawing of the PET films

When a polymer material is deformed *via* the crazing mechanism, the formed porous structure of the solvent-crazed polymer appears to be loaded with the surrounding liquid medium. Penetration of the macromolecules into the nanoporous structure of the PET assisted by the drawing deformation was judged by the measured PEO content in the crazed material. The profiles of PEO4K (curve 1) and PEO40K (curve 2) content from the 20% solutions as a function of the tensile strain are shown in Fig. 4. Curves 3 and 4 in the same plot represent the theoretical estimations of the amount of PEO4K and PEO40K, respectively, calculated from the experimental data on the PET porosity assuming that PEO concentration in the solution filling the pores is equal to that in the external solution.

Analysis of the data in Fig. 4 revealed the following peculiarities of PEO penetration into the nanoporous structure of crazed PET. (1) Over the whole range of tensile strain, PEO could penetrate into the nanoporous structure of the crazed PET irrespective of the molecular mass of PEO. (2) Over the whole range of tensile strain, the PEO content in the solvent-crazed PET being crazed was higher than the theoretically calculated one. That was in line with the earlier observations[32] for the blends based on PET crazed by 100% (in the strain range corresponding to the stable structure of crazes) in solutions of PEO with a molecular mass of 4×10^4–1×10^6. Taking into account the large specific surface of the fibrillized

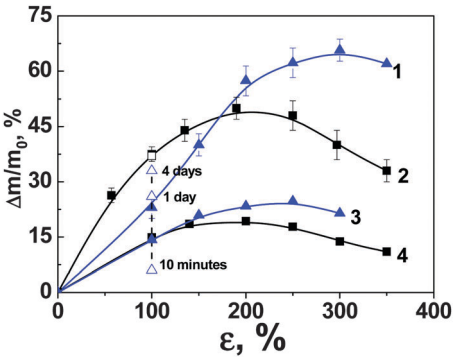

Fig. 4 The measured (1 and 2) and calculated (3 and 4) content of PEO4K (1 and 3) and PEO40K (2 and 4) in the solvent-crazed PET at the drawing rate of 5.4 mm min^{-1} in the 20% solution of the corresponding polymer as a function of the tensile strain. Open markers point at the PEO content during penetration of the pre-formed crazed PET matrix with the 20% solution of PEO4K (triangles) and PEO40K (squares); the numbers near the open markers show the penetration duration.

polymer (>100 m^2 g^{-1}) in the crazes and the high adsorbability of PEO on both hydrophobic and hydrophilic surfaces, it was assumed that PEO was adsorbed on the surface of the fibrillized material. (3) The profiles of PEO content as a function of the tensile strain were different for PEO4K and PEO40K (*cf.* curves 1 and 2 in Fig. 4).

3.4 Peculiarities of PEO penetration into the nanoporous structure of the solvent-crazed PET samples stretched by a tensile strain of 100–150%

We begin our analysis of the mechanism of PEO penetration into the nanoporous structure with a discussion of the PEO content during the initial stage of PET deformation (stretching up to 150%). The data in Fig. 4 show that the content of PEO in the obtained blends increased with the growing molecular mass of the penetrating macromolecules. The difference can be fairly substantial (*cf.* Fig. 4, data corresponding to the strain of 100%).

What is the reason for such a difference? As can be seen from Fig. 2, the PET porosity was almost independent of the PEO molecular mass over the discussed strain range. Therefore, the observed variation of PEO contents in the blends should be most reasonably assigned to the different adsorbability of PEO4K and PEO40K at the highly developed surface of the fibrillized polymer in the crazes rather than to the material porosity. The assumption was in accordance with the available data stating that the adsorption of polymers at smooth surfaces increases with their molecular mass.[43]

Another possible explanation of the observed difference in the content of PEO in the crazed PET as a function of the penetrating molecule molecular mass could be associated with different mechanisms of penetration of PEO.

Let us further analyze the data in Fig. 4. From the scheme in Fig. 1 we could conclude that the 20% solutions of PEO4K and PEO40K existed in the different concentration regimes. The PEO40K solution was semidilute entangled, whereas the PEO4K solution was semidilute unentangled. According to the scaling

 This journal is © the Owner Societies 2016

concept, the blobs of the size determined by the correlation length ξ[40] should be considered as the kinetic units in the elementary stages of the flexible-chain polymer transport in the semidilute entangled solutions (PEO40K), whereas macromolecules as a whole acted as such kinetic elements in the case of unentangled semidilute solutions (PEO4K). Macromolecules can penetrate into nanoporous materials, provided that a pore diameter is larger than either ξ or R_h. From Table 1 it follows that in the cases of both PEO40K (ξ = 0.8 nm) and PEO4K (R_h = 1.3 nm) there were no restrictions of PEO penetration in the pores with the effective diameter of about 7–8 nm (Table 2).

However, the data in Fig. 4 revealed that at the same tensile strain of PET (up to 150%), PEO4K content in the material was below that of PEO40K. According to the reference data, the structure of crazed polymers exhibits the distribution of the pore size even in the region of the stable crazes. Penetration in the smaller pores of the material could be restricted for PEO4K rather than for PEO40K. In addition to the variation in the adsorption strength, the pore distribution could be a factor determining the different content of PEO4K and PEO40K in the material prepared *via* deformation of PET in the PEO solution of the same concentration.

The reason for the observed difference could be elucidated taking into account the results of additional experiments attempting to change the diffusion mechanism of 20% PEO4K solution from the translation to the reptation. To do so, the PET specimens were deformed to the strain of 100% in the PEO-free water–ethanol mixture and then transferred to the 20% PEO4K solution in order to induce the concentration gradient-induced diffusion of PEO into the nanoporous structure of crazes. According to the data in Fig. 2, the porosity of such native specimens of PET was equal to that of the specimen deformed in the PEO4K solution and to the theoretically estimated one. However, direct penetration of PEO4K in the course of PET crazing occurred *via* the translation mechanism, whereas it was changed to the reptation one (typical of the diffusion process) in the case of the preliminary crazing. A blob acts as a kinetic element in the diffusion process instead of the macromolecule,[40] the blob being much smaller than the macromolecule hydrodynamic coil (Table 1). The dashed line in Fig. 4 marks the kinetic data on penetration of the pre-crazed PET specimens with PEO4K and PEO40K 20% solutions. The amount of PEO40K incorporated into the pre-crazed porous PET matrix *via* diffusion was equal to the corresponding content measured during the direct drawing of PET in the polymer solution. In other words, the amount of PEO40K penetrating into the PET matrix was independent of the method used, since in both cases the penetration occurred *via* the reptation mechanism. It was to be seen that the penetration of PEO *via* diffusion was slower than the direct penetration *via* crazing. In the case of PEO4K diffusion in the pre-crazed matrix, the content of the incorporated polymer was higher than that in the case of the penetration accompanying the crazing, and was almost equal to the content of PEO40K in the similar experiment.

Hence, additional experiments led to the conclusion that the observed difference in the penetration of PEO into the PET matrix being deformed to the strain of 100% in the solutions of PEO4K and PEO40K of the same concentration was mainly due to the change of the penetration mechanism and the presence of certain pore size distribution in the sample.

3.5 Peculiarities of PEO penetration into the nanoporous structure of the solvent-crazed PET samples stretched by a tensile strain of above 150%

Let us now consider the data on PEO4K and PEO40K penetration in the PET matrix being deformed to larger tensile strains (above 150%). The most important feature to be noticed is the different behavior observed during the deformation of PET in the solutions of PEO of the same concentration (20%) but differing in the molecular mass. In the case of PEO40K, the PEO content passed through a maximum as the strain was increased, whereas in the case of PEO4K the amount of the polymer penetrated into the matrix was increasing over the whole range of the considered strains (Fig. 4). Let us discuss the factors affecting the content of PEO40K in the PET deformed to high tensile strains.

Noteworthily, the content of PEO40K in the PET varied with the tensile strain coinciding with the respective plot of the native porosity of the crazed polymer (*cf.* Fig. 2 and 4). Obviously, that the decrease of the porosity and the PEO content observed when PET was drawn in the PEO solutions to high tensile strain reflected the structural rearrangements in the fibrillar-porous structure of the crazed polymer.

As has been noted above, the highly disperse fibrillar-porous structure of the crazes is thermodynamically unstable and tends to reduce the excess surface energy. As the tensile strain was increased, the fibrils connecting the opposite walls of crazes grew longer, thereby making the fibrils more flexible, facilitating the formation of coagulation contacts between them, and leading to the collapse of their fibrillar-porous structure. Consequently, the porosity of the deformed polymer inside the crazes was decreased (Fig. 2). Collapse (as well as syneresis) is accompanied by the partial escape of the liquid phase.[24,36] Since the liquid phase was a polymer solution, the collapse was accompanied by the release of PEO solution into the external medium. In other words, the PEO mass transfer was reversed, and penetration of PEO at the initial stage of deformation (pore development) turned into the release at the later stage (the porous structure collapse). However, the polymer still contained a fairly large fraction of the initial non-deformed polymer fragments at the onset of the porous structure collapse (Fig. 3, stage IV), localized between the crazes and being in contact with the AAM under the conditions of mechanical load. Those fragments were further crazed; as a result, additional portions of PEO penetrated into the crazed PET. Therefore, the total content of PEO in the polymer deformed to larger tensile strains (Fig. 4) is determined by the two opposite processes: release of the PEO solution due to the structural rearrangements in the crazes and its penetration into the matrix owing to the ongoing crazing of the non-deformed parts of the polymer.

As has been mentioned above, the content of PEO40K in the crazed polymer exceeded that calculated under the assumption of the pores filled with the external solution over the whole

studied range of PET deformation (Fig. 4). It could be therefore suggested that the diphilic PEO was adsorbed at the well developed surface of the fibrillized polymer in the crazes. Based on the available reference data,[44–48] the structure of the adsorbed PEO was expected to depend on its molecular mass and concentration in the solution. Evidently, the lower concentration and the smaller molecular mass should facilitate the planar conformation of the macromolecules adsorbed at the fibril surface and improve the contact between the flexible-chain macromolecule and the matrix; *vice versa*, at high concentration and high molecular mass the flexible-chain polymer should suppress its contact with the matrix surface due to the less planar conformation.[49,50] Hence, the PEO4K macromolecules should be more strongly bound to the fibril surface as compared to the PEO40K ones due to the different conformation, and pushing out of PEO4K macromolecules from the craze structure upon its collapse should be suppressed.

As has been stated above, the content of PEO4K and PEO40K from the solutions of the same concentration was different at high tensile strain of the deformed PET (>150%). Porosity of the PET deformed in the solutions of PEO4K was higher and tended to increase up to the higher strain value (Fig. 2). That could show the stronger stabilization of the crazes against collapse at high tensile strength assisted by PEO4K.

Let us now consider the porosity and PEO content data at high deformations in the presence of PEO4K in the external solution. The measured porosity deviated from the theoretically calculated values at a strain of above 150%; however, it further grew to reach a maximum at the strain of 250% and decreased at the strain of 300% (Fig. 2). The described trend evidenced about the collapse process occurring in the course of PET deformation in the PEO4K solutions. At the same time, the PEO4K content in the PET was continuously increasing with the tensile strain up to 300% deformation (Fig. 4). Even though the increasing PEO4K content in the mid-range of the tensile strain could be explained by the simultaneous opposite processes of partial pushing out of the PEO4K solution (due to the collapse) and additional PEO penetration in the matrix pores (ongoing crazing in the pristine parts of the PET). However, such explanation was invalid for the data at around a strain of 300%, since simultaneous decrease of the porosity and increase of PEO4K content were observed. The only reasonable explanation of such unexpected behavior was pushing the pure solvent (AAM) out of the collapsing matrix, whereas PEO4K remained trapped in the collapsed matrix structure. The hypothesis was plausible, since the collapse induced the decrease of the effective pore diameter (Table 2), and at the strain of 300% the pore size turned comparable to the hydrodynamic radius of PEO4K.

What factor gave the major contribution to the difference in the behavior of PET in the course of its crazing in the PEO40K and PEO4K solutions? That could be deduced from data in Fig. 5A showing the PEO content by the PET matrix being deformed in the solutions at different concentrations of the same molecular mass polymer (PEO40K). Curve 2 in that figure corresponds to the 20% solution and has been discussed above in detail; curve 1 shows similar data for the 5.5% PEO40K solution. Those concentrations corresponded to the different solution regimes: the 20% solution of PEO40K was semidilute entangled, and the 5.5% one was semidilute unentangled. Therefore, the penetration of PEO40K in the crazes aided by the negative hydrodynamic pressure occurred *via* the reptation and the translation mechanisms, respectively. In turn, that led to the different profiles of the PEO content under the studied conditions. In the case of the 20% PEO40K solution the shape of the corresponding curve was "classical": the PEO content initially grew up with the tensile strain to reach the maximum and further decreased at the larger strains corresponding to the collapse stage. In the case of the 5.5% solution of PEO40K, its content grew linearly with the deformation over the whole studied strain range.

Hence, we concluded that the different behavior of the 20% solutions of PEO40K and PEO4K was due to the different mechanism of PEO penetration into the PET structure.

Finally, Fig. 5B displays similar data for the PEO4K dilute (1), semidilute unentangled (2) and entangled (3) solutions.

The first two curves exhibited the continuous increase of PEO content, typical of the solutions with the translation mechanism of the flow and penetration in the pores. The 30% solution of PEO4K showed an unexpected trend over the large strain range, since no maximum was observed under the conditions corresponding to the structure collapse (however, the PEO content with deformation was somewhat lower at the strains of above 200%, evidencing the possible squeezing out of the polymer). Nevertheless, the amount of PEO pushed out due to the collapse was less than that penetrated inside the matrix due to the ongoing crazing of the pristine parts of PET. Such behavior of the 30% PEO4K solution (the kinetic element

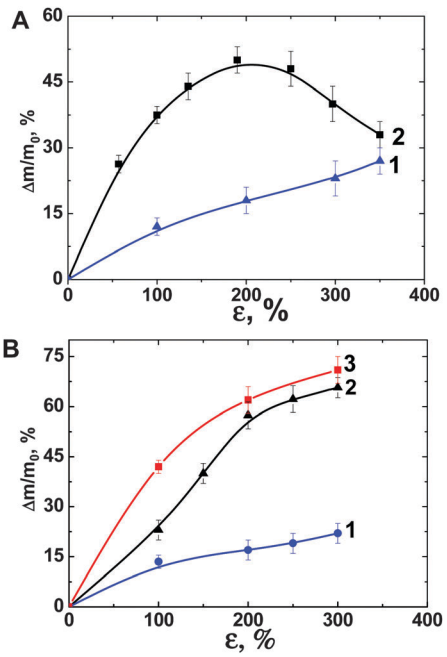

Fig. 5 PEO40K (A) and PEO4K (B) content in the PET matrix deformed in the 5.5 (1), 20 (2) and 30% (3) solutions at a rate of 5.4 mm min^{-1} as a function of the tensile strain.

This journal is © the Owner Societies 2016

corresponding to the reptation mechanism of the flow was sufficiently small and could not prevent the polymer pushing out, *cf.* Tables 1 and 2) has not been unambiguously explained at this moment. A possible explanation could be related to the above-mentioned strong stabilizing action of PEO4K against the collapse processes. The observed effect requires further investigation.

4. Conclusions

The study of PET crazing in the PEO solutions (differing in the concentration and the molecular mass of the flexible-chain polymer) revealed that PEO could penetrate into the nanoporous PET structure over the whole range of tensile strains used. The two ranges of tensile strain could be distinguished: that of small ($<150\%$) and large ($>150\%$) deformations, corresponding to the different profiles of PEO content in the PET matrix. At the lower strains, the PEO content was continuously increased with the deformation, accompanied by the porosity increase. At the larger strains the crazing of pristine non-deformed parts of the polymer matrix occurred simultaneously with the collapse of the fibrillar-porous structure of the crazes. Therefore, at high strain PEO could simultaneously penetrate into the freshly formed porous regions and be pushed out of the collapsing parts of the structure (syneresis). Since the collapse was accompanied by both the decrease of the overall porosity and the pore diameter, the PEO content as a function of the strain could exhibit a complex shape. In particular, the PEO content in the deformed PET matrix was affected by both the PEO molecular mass and concentration in the solution, being related to the flow mechanism (reptation or translation).

Acknowledgements

This work was financially supported by the Russian Foundation for Basic Research (project no. 15-03-03430_a). The authors would like to thank E. A. Karpushkin, for assisting with preparation article.

References

1 A. A. Kurganov, F. Svec and A. Y. Kanateva, *Polymer*, 2015, **60**, A1–A18.
2 G. Guillot, *Macromolecules*, 1987, **20**, 2600–2606.
3 L. Li, Q. Chen, F. Jin and C. Wu, *Polymer*, 2015, **67**, A1–A13.
4 *Polymers in Confined Environment*, ed. S. Granick, Springer-Verlag, Berlin, 1999.
5 L. Movileanu, S. Cheley and H. Bayley, *Biophys. J.*, 2003, **85**, 897–910.
6 T. Sakaue and E. Raphael, *Macromolecules*, 2006, **39**, 2621–2628.
7 J. Lal, S. K. Sinha and L. Auvray, *J. Phys. II*, 1997, **7**, 1597–1615.
8 K. Shin, S. Obukhov, J.-T. Chen, J. Huh, Y. Hwang, S. Mok, P. Dobriyal, P. Thiyagarajan and T. P. Russell, *Nat. Mater.*, 2007, **6**, 961–965.
9 H. Grull, R. Shaulitch and R. Yerushalmi-Rozen, *Macromolecules*, 2001, **34**, 8315.
10 Y. G. Mishael, P. L. Dubin, R. de Vries and A. B. Kayitmazer, *Langmuir*, 2007, **23**, 2510–2516.
11 I. Teraoka, Z. Zhou, K. H. Langley and F. E. Karasz, *Macromolecules*, 1996, **29**, 37–43.
12 M. Ladero, A. Santos and F. Garcia-Ochoa, *Chem. Eng. Sci.*, 2007, **62**, 666–678.
13 E. V. Khataibe, T. D. Khokhlova, L. I. Trusov and B. V. Mchedlishvili, *Colloid J.*, 2005, **67**, 124–127.
14 P. Y. Apel, I. V. Blonskaya, O. L. Orelovich, S. N. Akimenko, B. Sartowska and S. N. Dmitriev, *Colloid J.*, 2004, **66**, 725–732.
15 Y. Caspi, D. Zbaida, H. Cohen and M. Elbaum, *Macromolecules*, 2009, **42**, 760–767.
16 J. Shao and R. E. Baltus, *AIChE J.*, 2000, **46**, 1149–1156.
17 L. Beguin, B. Grassl, F. Brochard-Wyart, M. Rakib and H. Duval, *Soft Matter*, 2011, **7**, 96–103.
18 O. V. Krasilnikov, C. G. Rodrigues and S. M. Bezrukov, *Phys. Rev. Lett.*, 2006, **97**, 018301.
19 G. Yu, W. Cho and K. Shin, in *Adsorption and Phase Behaviour in Nanochannels and Nanotubes*, ed. L. J. Dunne and G. Manos, Springer, London, New-York, 2009, ch. 5, p. 101.
20 C. C. Hsie and P. S. Doyle, *Korea-Aust. Rheol. J.*, 2008, **20**, 127–142.
21 A. Taloni, J.-W. Yeh and C.-F. Chou, *Macromolecules*, 2013, **46**, 7989–8002.
22 L. Dai, S. Y. Ng, P. S. Doyle and J. R. C. van der Maarel, *ACS Macro Lett.*, 2012, **1**, 1046–1050.
23 C. Zhang, D. Guttula, F. Liu, P. P. Malar, S. Y. Ng, L. Dai, P. S. Doyle, J. A. van Kan and J. R. C. van der Maarel, *Soft Matter*, 2013, **9**, 9593–9601.
24 A. L. Volynskii and N. F. Bakeev, *Solvent Crazing of Polymers*, Elsevier, Amsterdam, New-York, 1995.
25 H. H. Kausch and A. S. Argon, *Crazing in Polymers: vol. 2*, Springer-Verlag, Berlin, New York, 1990.
26 R. P. Kambour, *J. Polym. Sci., Macromol. Rev.*, 1973, **7**, 1–154.
27 A. V. Volkov, A. A. Tunyan, M. A. Moskvina, A. I. Dement'ev, N. G. Yaryshev, A. L. Volynskii and N. F. Bakeev, *Polym. Sci., Ser. A*, 2011, **53**, 158–165.
28 E. S. Trofimchuk, N. I. Nikonorova, E. A. Nesterova, A. S. Eliseev, E. V. Semenova, I. B. Meshkov, V. V. Kazakova, A. M. Muzafarov, A. L. Volynskii and N. F. Bakeev, *Polym. Sci., Ser. A*, 2007, **49**, 1107–1113.
29 A. L. Volynskii, L. M. Yarysheva and N. F. Bakeev, *Fibre Chem.*, 2006, **38**, 138–141.
30 E. G. Rukhlya, L. M. Yarysheva, A. L. Volynskii and N. F. Bakeev, *Polym. Sci., Ser. B*, 2007, **49**, 245–246.
31 L. M. Yarysheva, O. V. Arzhakova, A. A. Dolgova, A. L. Volynskii, E. G. Rukhlya and N. F. Bakeev, *Int. J. Polym. Anal. Charact.*, 2007, **12**, 65–75.
32 E. G. Rukhlya, E. A. Litmanovich, A. I. Dolinnyi, L. M. Yarysheva, A. L. Volynskii and N. F. Bakeev, *Macromolecules*, 2011, **44**, 5262–5267.

33 A. L. Volynskii, E. G. Rukhlya, L. M. Yarysheva and N. F. Bakeev, *Dokl. Phys. Chem.*, 2012, **447**, 200–202.
34 A. Yarysheva, D. Bagrov, E. Rukhlya, L. Yarysheva, A. Volynskii and N. Bakeev, *Polym. Sci., Ser. A*, 2012, **54**, 779–786.
35 A. L. Volynskii, A. Y. Yarysheva, E. G. Rukhlya, L. M. Yarysheva and N. F. Bakeev, *Dokl. Phys. Chem.*, 2014, **454**, 1–4.
36 A. L. Volynskii and N. F. Bakeev, *Polym. Sci., Ser. C*, 2005, **47**, 74–100.
37 L. M. Yarysheva, N. B. Galperina, O. V. Arzhakova, A. L. Volynskii, N. F. Bakeev and P. V. Kozlov, *Polym. Sci., Ser. B*, 1989, **31**, 211–216.
38 U. Zettl, S. T. Hoffmann, F. Koberling, G. Krausch, J. Enderlein, L. Harnau and M. Ballauff, *Macromolecules*, 2009, **42**, 9537–9547.
39 A. V. Dobrynin, R. H. Colby and M. Rubinstein, *Macromolecules*, 1995, **28**, 1859–1871.
40 P. G. de Gennes, *Scaling Concepts in Polymer Physics*, Cornell University Press, Ithaca, New York, 1979.
41 Y.-J. Shenga and M.-C. Wang, *J. Chem. Phys.*, 2001, **114**, 4724–4729.
42 M. Doi and S. F. Edwards, *The Theory of Polymer Dynamics*, Clarendon, Oxford, U.K., 1986.
43 J. Koral, R. Ullman and F. R. Eirich, *J. Phys. Chem.*, 1958, **62**, 541–550.
44 Y. Cohen and A. B. Metzner, *Macromolecules*, 1982, **15**, 1425–1429.
45 *Encyclopedia of Surface and Colloid Science*, ed. P. Somasundaran, Taylor & Francis, New York, 2006.
46 M. A. C. Stuart and G. J. Fleer, *Annu. Rev. Mater. Sci.*, 1996, **26**, 463–500.
47 A. N. Semenov, J. Bonet-Avalos, A. Johner and J. F. Joanny, *Macromolecules*, 1996, **29**, 2179–2196.
48 W. van Bronswijk, L. J. Kirwan and P. D. Fawell, *Vib. Spectrosc.*, 2006, **41**, 176–181.
49 G. Zhang and R. Seright, *SPE J. (Soc. Pet. Eng.)*, 2014, **19**, 373–380.
50 C. Peterson and T. K. Kwei, *J. Phys. Chem.*, 1961, **65**, 1330–1333.

 This journal is © the Owner Societies 2016